Available online at www.sciencedirect.com

ScienceDirect

Procedia Structural Integrity 25 (2020) 47–54

Structural Integrity Procedia

www.elsevier.com/locate/procedia

1st Virtual Conference on Structural Integrity - VCSI1

Poly(Methyl Methacrylate) Structure Modification through Zn-Cu-In-S / ZnS Quantum Dot Nanocrystals Dispersion

George Saatsakis[a], Christos Michail[b,*], Christina Fountzoula[c], Athanasios Bakas[c], Nektarios Kalyvas[b], Konstantinos Ninos[c], George Fountos[b], Ioannis Kandarakis[b], Ioannis Valais[b] and George Panayiotakis[a]

[a]*University of Patras, School of Medicine, Department of Medical Physics, GR-15310, Rion, Greece*
[b] *Radiation Physics, Materials Technology, and Biomedical Imaging Laboratory, University of West Attica, Department of Biomedical Engineering, 122 10 Athens, Greece*
[c] *University of West Attica, School of Biomedical Sciences, 122 10 Athens, Greece*

Abstract

The aim of the current study was to present a simple method for the fabrication of quantum dot (QD)/polymer films for possible use as a luminescent material in medical applications. To this aim the poly(methyl methacrylate) (PMMA) polymer matrix was modified in order to host Zinc Copper Indium Sulfide encapsulated by an outer core of Zinc Sulfide (ZnCuInS/ZnS) QD nanocrystals, through dispersion. Four composite PMMA films of ZnCuInS/ZnS nanocrystals with maximum emission at 530 nm and concentrations of 1.0, 4.0, 6.0 and 10.0 %w/v, were prepared. X-ray irradiation and scanning electron microscopy (SEM) micrographs were used to evaluate the volume homogeneity of the final samples, as a measure of QD dispersion. The coefficient of variation (CV) estimated from homogeneity measurements, increased with increasing concentration, for the 1.0, 4.0 and 6.0 %w/v samples. The minimum CV value was obtained for the 10.0 %w/v sample which is attributed to the incorporation of sonication in the final product, during the fabrication process. Homogenous dispersion was observed from the SEM micrographs.

* Corresponding author. Tel.: +0-000-000-0000 .
E-mail address: michail@upatras.gr

2452-3216
10.1016/j.prostr.2020.04.008

Keywords: PMMA; Quantum Dots; ZnCuInS/ZnS; UV; polymer matrix

1. Introduction

QDs are inorganic semiconductor nanocrystals with sizes ranging from 2-10nm (Feng et al. 2019; Saatsakis et al. 2019a). During fluorescence stimulation, quantum dots are excited by radiation of specific energy and emit in different wavelengths, depending on their size (Zych et al. 2003; Kim et al. 2007; Ganesan et al. 2018; Saatsakis et al. 2019b). Their excellent chemical and physical properties, such as the high energy conversion efficiency, the high extinction coefficient, tunable emitting wavelength, the broad excitation spectrum, and the resistance to photobleaching have attracted the interest of the scientific community providing quite impressive results (Konstantatos et al. 2007; Del Sordo et al. 2009; Rauch et al. 2009; Stodilka et al. 2009; Baharin et al. 2010; Konstantatos and Sargent 2011; Öberg et al. 2017). QDs are 20 times brighter and 100 times more stable than traditional fluorescent indicators (Chan 1998). During the last years, QDs have been employed in many areas like solar cells, transistors, LEDs, medicine and biology applications, as well as, quantum computing (Giepmans et al. 2005; Michalet 2005; Yu et al. 2006; Jamieson et al. 2007; Luo et al. 2011; Lawrence et al. 2012; Son et al. 2012; Fiaczyk and Zych 2016; Nikolopoulos et al. 2016; Zeler et al. 2016; Saatsakis et al. 2017; Wu et al. 2018; Saatsakis et al. 2019b).

QDs that contain Cadmium or Mercury have been used in the above areas; however, for biomedical applications, QDs must meet additional criteria since toxic compounds are not allowed. Under the prism of nontoxicity, Cadmium free Zinc Copper Indium Sulfide encapsulated by an outer core of Zinc Sulfide (ZnCuInS/ZnS) QDs might be an interesting candidate for medical applications (RoHS 2014; Saatsakis et al. 2019c). Another important factor which dictated the use of ZnCuInS/ZnS QDs was the fact that they emit light in the green region of the optical spectrum, being compatible with the most common digital optical sensors which are utilized in biomedical instrumentation (Michail et al. 2010; Michail et al. 2018a; Michail et al. 2018b; Michail et al. 2019). Multiple methods have reported for the preparation of QD films (Seferis et al. 2016; Dong et al. 2017; Martini et al. 2018; Seferis et al. 2018; Martini et al. 2019; Anastasiou et al. 2020). Previous work of our group introduced a simple method for the fabrication of composite films using a mixture of powder scintillators and Polymethyl methacrylate (PMMA) (Valais et al. 2017a). PMMA is a well-known thermoplastic which is widely used in biomedical applications (Allcock et al. 2003; Balamurugan et al. 2004; Valais et al. 2017b; Michail et al. 2018b). Various fatigue experiments have been carried in order to examine the structural integrity of PMMA polymers for various applications (Domínguez Almaraz et al. 2017; Okeke et al. 2019). The in vitro and in vivo biocompatibility of PMMA has been studied extensively and its resins are broadly used in medicine (Thomson et al. 1992). In ophthalmology, intraocular lenses are made of PMMA while in orthopedic surgery PMMA is used as bone cement in joint replacements, screw fixation in bone and filler for bone cavities and skull defects (Thomson et al. 1992; Hollick et al. 1999). Also, in dentistry PMMA is used in dental prostheses (Gautam et al. 2012; Huettig et al. 2016; Domínguez Almaraz et al. 2017). In this study, the PMMA polymer matrix host was modified in order to incorporate ZnCuInS/ZnS QD nanocrystals, for possible use in medical applications.

Fabrication of compound films with layers of different QD concentrations could affect the optical properties of the compound films, i.e. refractive index, back scattering, etc., as was depicted in previous studies (Chen et al. 2008; Kumar et al. 2017), lead to the minimization of the reflected UV radiation, thus, increase the amount of radiation that contributes to the production of luminescent light. To this aim, different concentrations of the QDs were dispersed within the polymer matrix. Volume homogeneity as a measure of QD dispersion of the composite films was assessed using medical X-ray images and scanning electron microscopy (SEM) micrographs.

2. Materials and Methods

PMMA (Poly Methyl MethAcrylate) powder (average Mw ~120000 by GPC) and liquid MMA monomer were purchased from Sigma- Aldrich and Alfa Aesar respectively, both with purities reaching 99%. PMMA and MMA were mixed in a ratio of 1:2.5 (Valais et al. 2017) in order to produce a slurry, with optimum viscosity for further handling and processing. ZnCuInS/ZnS QDs (particle size: 5 nm, emission wavelength: 530±15nm, cadmium free,

hydrophobic) were purchased from PlasmaChem GmbH in powder form. Different amounts of QD (25, 100, 150 and 250 mg) were diluted in 1 mL toluene (Fluka Chemica, purity >99%). The dilution process was facilitated using an ultrasonic bath (TRITON – TR USR070) and a vortex (Velp Scientifica Zx3) (Figure 1).

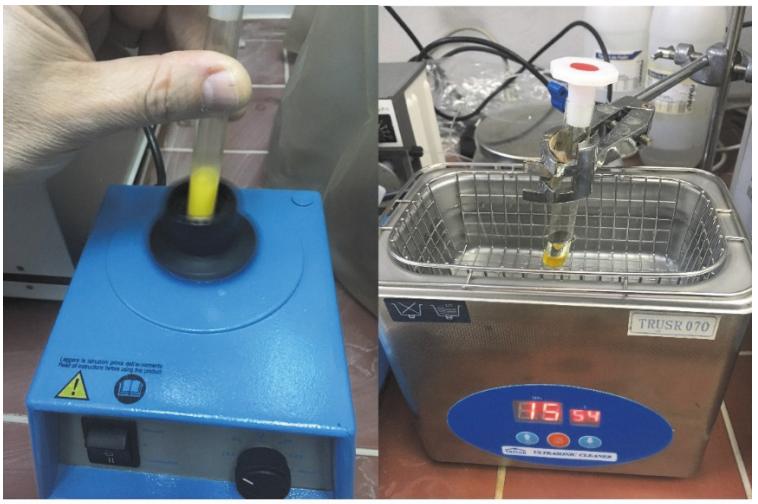

Fig. 1. Vortex (Velp Scientifica Zx3) and ultrasonic bath (TRITON – TR USR070) for the dilution process.

Furthermore, 1.5 mL of the slurry PMMA/MMA was introduced in each QD solution, followed by vortex stirring. The final product of QD concentrations, namely: 25, 100 and 150 mg was poured into flexible silicone molds while the final product of QD concentration 250 mg underwent sonication for 5 minutes before it was poured into a flexible silicone mold too.

Molds filled with the final products were put under vacuum for 15 minutes to remove entrapped air bubbles from the mixture. Removal of any residual solvent was accomplished by putting the samples in a vacuum oven (Vaciotem T, model 4001489) for 24h at 50 °C. The produced samples were labeled as QD25 (25mg QD/mL toluene, 1.0 %w/v in QD), QD100 (100mg QD/mL toluene, 4.0 %w/v in QD), QD150 (150mg QD/mL toluene, 6.0 %w/v in QD) and QD250 (250 mg QD/mL toluene, 10.0 %w/v in QD), whereas the QD number indicates the amount of QD in milligrams within the sample (Figure 2).

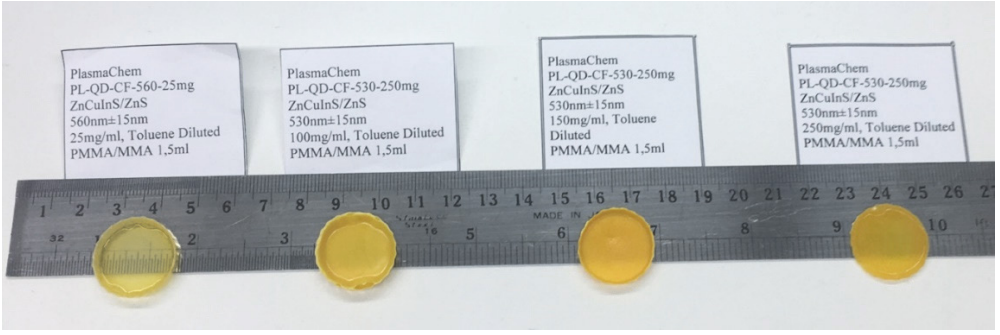

Fig. 2. The produced compound films samples, from left to right: QD25 (25mg QD/mL toluene, 1.0 %w/v in QD), QD100 (100mg QD/mL toluene, 4.0 %w/v in QD), QD150 (150mg QD/mL toluene, 6.0 %w/v in QD) and QD250 (250 mg QD/mL toluene, 10.0 %w/v in QD).

3. Results and Discussion

The X-ray images were acquired from the Siemens Mammomat Inspiration mammography unit with 32 KV tube voltage and 8 mAs tube current product, providing a dose of 0.4807 mGy (Figure 3). The mammography unit incorporates a direct-to-digital amorphous selenium (a-Se) detector with dimensions of 24 cm x 30 cm. The X-ray tube anode material is Molybdenum and Tungsten (Mo/W) and the filter Molybdenum and Rhodium (Mo/Rh). The source to detector distance (SDD) is 65 cm.

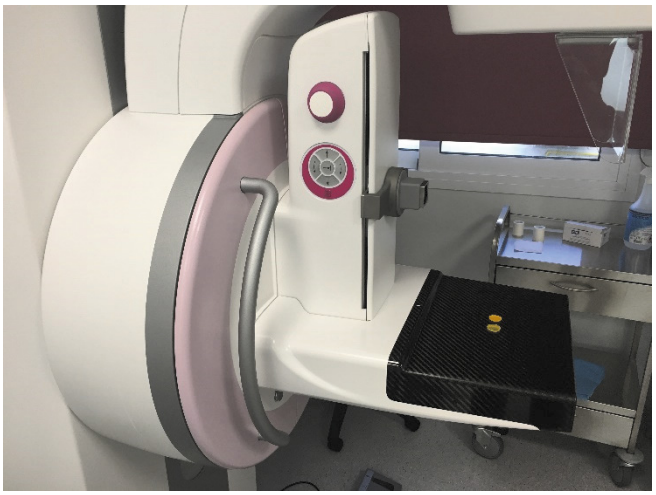

Fig. 3. The produced compound films samples on the Mammography X-ray unit.

Figures 4 and 5 show the resulted X-ray images of the compound polymer films that were obtained in order to assess the volume homogeneity as a result of Zinc Copper Indium Sulfide encapsulated by an outer core of Zinc Sulfide QD dispersion. Excellent PMMA homogeneity achieved; however, the formation of QD clusters as a result of aggregations was also revealed. QD25, QD100, and QD150 developed a significant amount of QD clusters while QD250 performed much better due to the use of sonication. QD aggregations are apparent in the compound films QD100 and QD150. Even though the fabrication process to produce the QD25 sample was identical, aggregations in this sample are not macroscopically visible due to the small QD concentration. The 5 minutes sonication during fabrication process diminished aggregations in the sample with the highest QD concentration (QD250).

Table 1 shows the coefficient of variation (CV) values calculated as the ratio of the standard deviation to the mean. The CV values increases as the QD concentration increases while for the QD250 sample the CV value drops dramatically due to the 5 minutes sonication incorporated in the fabrication method.

Table 1. CV of the prepared ZnCuInS/ZnS/PMMA films.

Concentration (mg)	SD	CV
25	3.578	0.015796
100	5.365	0.026304
150	12.504	0.081544
250	6.328	0.047958

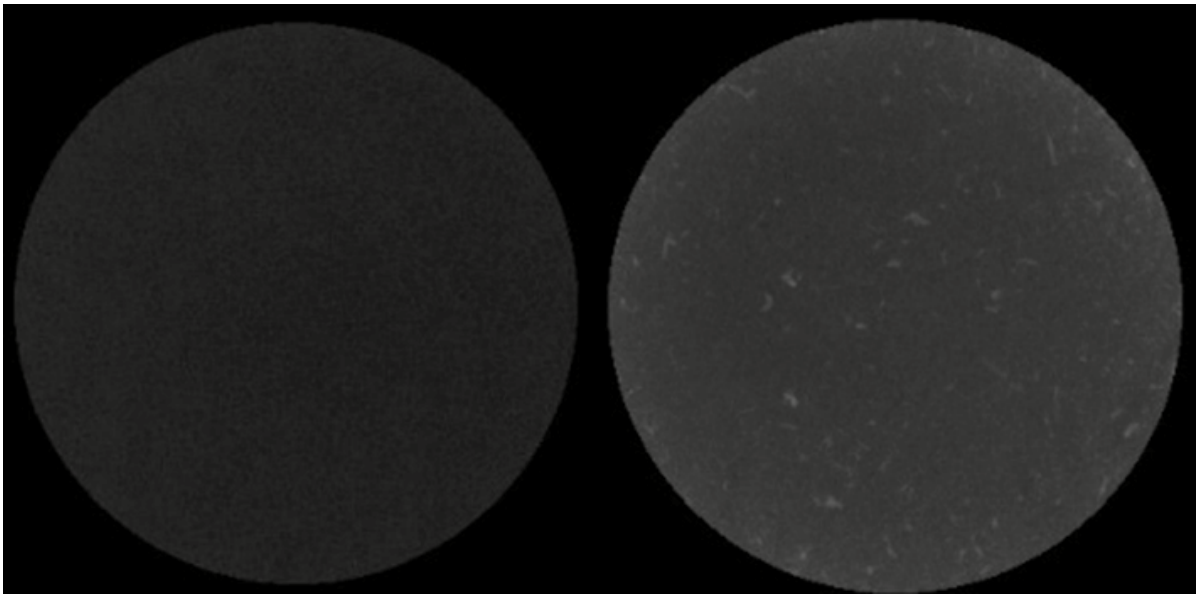

Fig. 4. X-ray imaging of the Q25 (left) and QD100 (right) compound films.

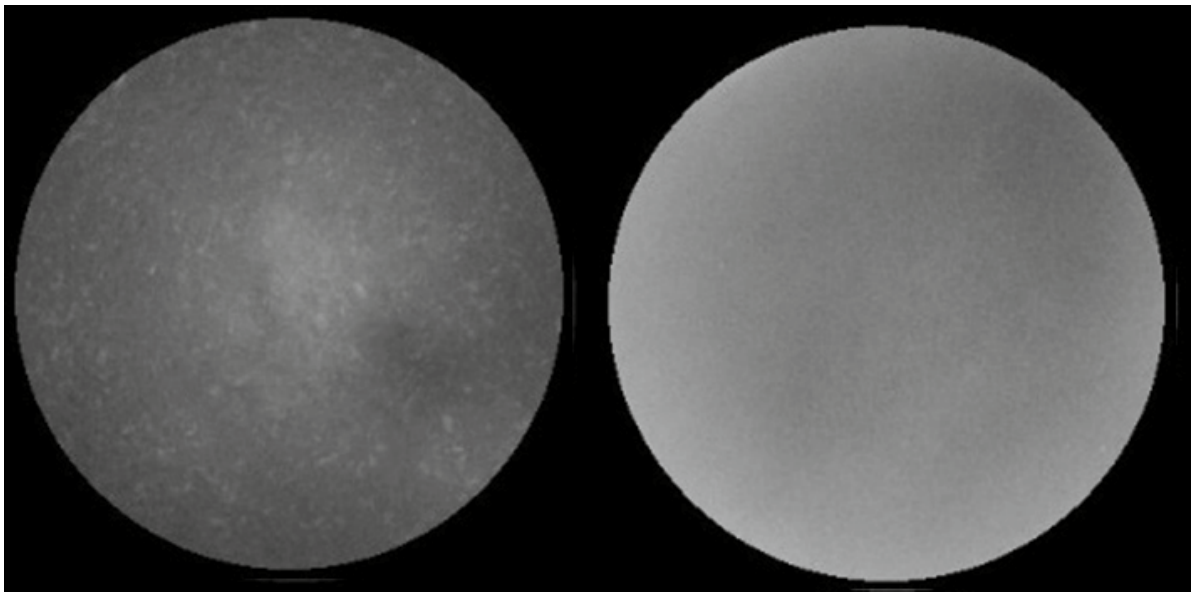

Fig. 5. X-ray imaging of the Q150 (left) and QD250 (right) compound films.

The thicker QD250 sample required SEM imaging despite the resolution limitations of SEM compared to transmission electron microscopy (TEM). A sample micrograph is shown in Figure 6. The CV was measured in each sample. In this image can be seen only a few aggregations. From this image homogenous QD dispersion can be observed, but we assume that an increased sonication time would lead to even better QD dispersion and fewer QD clusters. Excessive aggregation can lead to the formation of QD clusters which behave like energy traps and can trigger several excitation energy transfer processes, due to short interparticle distances, like FRET, etc. Photoluminescence quenching and energy trapping due to energy migration in the QD lattice has been well described (Martín-García et al. 2013; Alejo et al. 2017).

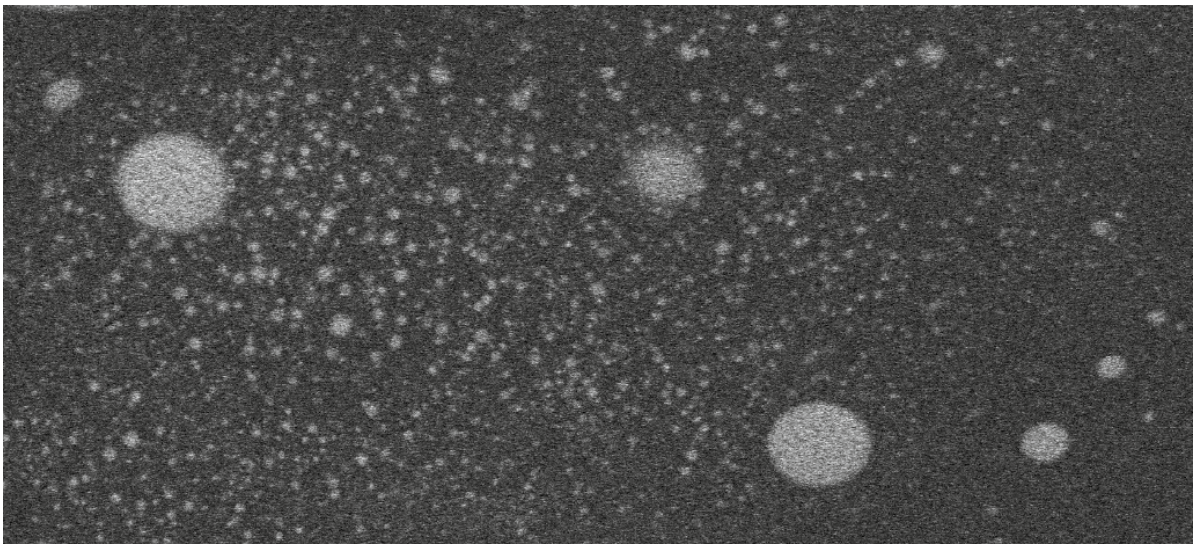

Fig. 6. SEM image of the QD250 sample.

4. Conclusions

In this research, we present a simple method for the fabrication of QDs/PMMA films. Homogeneity of the PMMA matrix and QDs dispersion was evaluated by means of X-ray irradiation. Excellent PMMA homogeneity was achieved; however, the formation of QD clusters as a result of aggregations was also revealed. The samples with concentrations 25, 100, and 150 mg developed a significant amount of QD clusters while the sample with concentration 250 mg performed much better due to the use of sonication process. Homogenous dispersion was observed from SEM microscopy. Our team is currently working on further optimization of the fabrication method including, pre-polymerization of MMA which could lead in minimization of QD clustering and better QD dispersion, as well as, on other parameters like the sonication and steering duration, polymerization temperature and the vacuum applied for the degassing process. Also, fabrication of QD/PMMA films with layers of different QD concentrations could minimize the reflected radiation, thus maximize the radiation contributed to luminescence.

References

Alejo, T., Paulo, P.M.R., Merchán, M.D., Garcia-Fernandez, E., Costa, S.M.B., Velázquez, M.M, 2017. Influence of 3D aggregation on the photoluminescence dynamics of CdSe quantum dot films. Journal of Luminescence, 183, 113-120.

Allcock, H.R., Bender, J.D., Chang, Y., McKenzie, M., Fone, M.M, 2003. Controlled Refractive Index Polymers: Polyphosphazenes with Chlorinated- and Fluorinated-, Aryloxy- and Alkoxy- Side-Groups. Chemistry of Materials, 15, 473-477.

Anastasiou, A., Papastamati, F., Bakas, A., Michail, C., Koukou, V., Martini, N., Lavdas, E., Valais, I., Fountos, G., Kandarakis, I, Kalyvas, N, 2020. Spatial frequency domain analysis of a commercially available digital dental detector. Measurrement, 151, 1071712019.

Baharin, R., Hobson, P.R., Smith, D.R, 2010. Simulation of MeV electron energy deposition in CdS quantum dots absorbed in silicate glass for radiation dosimetry. Journal of Physics: Conference Series, 245, 012007.

Balamurugan, A., Kannan, S., Selvaraj, V., Rajeswari, S, 2004. Development and Spectral Characterization of Poly (Methyl Methacrylate)/Hydroxyapatite Composite for Biomedical Applications. Trends in Biomaterials and Artificial Organs, 1841-1845.

Chan, W.C, 1998. Quantum Dot Bioconjugates for Ultrasensitive Nonisotopic Detection. Science, 281, 2016-2018.

Chen, J., Chen, X., Xu, R., Zhu, Y., Shi, Y., Zhu, X, 2008. Refractive index of aqueous solution of CdTe quantum dots. Optics Communications, 281, 3578-3580.

Del Sordo, S., Abbene, L., Caroli, E., Mancini, A.M., Zappettini, A., Ubertini, P, 2009. Progress in the Development of CdTe and CdZnTe Semiconductor Radiation Detectors for Astrophysical and Medical Applications. Sensors, 9, 3491-3526.

Domínguez Almaraz, G., Gutiérrez Martínez, A., Hernández Sánchez, R., Correa Gómez, E., Guzmán Tapia M., Verduzco Juárez J, 2017. Ultrasonic Fatigue Testing on the Polymeric Material PMMA, Used in Odontology Applications. Procedia Structural Integrity 3, 562-570.

Dong, X., Xu, J., Shi, S., Zhang, X., Li, L., Yin, S, 2017. Electroluminescence from ZnCuInS/ZnS quantum dots/poly(9-vinylcarbazole) multilayer films with different thicknesses of quantum dot layer. Journal of Physics and Chemistry of Solids, 104, 133-138.

Feng, Q., Wei, W., Zhang, B., Wang, H., Wang, J., Cong, H., Wang, T., Zhang, J, 2019. O-Band and C/L-Band III-V Quantum Dot Lasers Monolithically Grown on Ge and Si Substrate. Applied Sciences 9, 385.

Fiaczyk, K., Zych, E. On peculiarities of Eu^{3+} and Eu^{2+} luminescence in Sr_2GeO_4 host, 2016. RSC Advances, 6, 91836.

Ganesan, A.A., Houtepen, A.J., Crisp, R.W. Quantum Dot Solar Cells: Small Beginnings Have Large Impacts, 2018. Applied Sciences, 8, 1867.

Gautam, R., Singh, R.D., Sharma, V.P., Siddhartha, R., Chand, P., Kumar, R, 2012. Biocompatibility of polymethylmethacrylate resins used in dentistry. Journal of Biomedical Materials Research Part B: Applied Biomaterials, 100B, 1444-1450.

Giepmans, B.N.G., Deerinck, T.J., Smarr, B.L., Jones, Y.Z., Ellisman, M.H, 2005. Correlated light and electron microscopic imaging of multiple endogenous proteins using Quantum dots. Nature Methods, 2, 743.

Hollick, E.J., Spalton, D.J., Ursell, P.G., Pande, M.V., Barman, S.A., Boyce, J.F., Tilling, K, 1999. The effect of polymethylmethacrylate, silicone, and polyacrylic intraocular lenses on posterior capsular opacification 3 years after cataract surgery. Ophthalmology, 106, 49-55.

Huettig, F., Prutscher, A., Goldammer, C., Kreutzer, C.A., Weber, H, 2016. First clinical experiences with CAD/CAM-fabricated PMMA-based fixed dental prostheses as long-term temporaries. Clinical Oral Investigations, 20, 161-168.

Jamieson, T., Bakhshi, R., Petrova, D., Pocock, R., Imani, M., Seifalian, A.M, 2007. Biological applications of quantum dots. Biomaterials, 28, 4717-4732.

Kim, S., Park, J., Kang, S., Cha, B., Cho, S., Shin, J., Son, D., Nam, S, 2007. Investigation of the imaging characteristics of the Gd_2O_3:Eu nanophosphor for high-resolution digital X-ray imaging system. Nuclear Instruments and Methods in Physics Research Section A: Accelerators, Spectrometers, Detectors and Associated Equipment, 576, 70-74.

Konstantatos, G., Clifford, J., Levina, L., Sargent, E.H, 2007. Sensitive solution-processed visible-wavelength photodetectors. Nature Photonics, 1, 531-534.

Konstantatos, G., Sargent, E.H, 2011. Colloidal quantum dot photodetectors. Infrared Physics & Technology, 54, 278-282.

Kumar, V.B., Sahu, A.K., Mohsin, A.S.M., Li, X., Gedanken, A, 2017. Refractive-Index Tuning of Highly Fluorescent Carbon Dots. ACS Applied Materials & Interfaces, 9, 28930-28938.

Lawrence, W.G., Thacker, S., Palamakumbura, S., Riley, K.J., Nagarkar, V.V, 2012. Quantum Dot-Organic Polymer Composite Materials for Radiation Detection and Imaging. IEEE Transactions on Nuclear Science, 59, 215-221.

Luo, T., Huang, P., Gao, G., Shen, G., Fu, S., Cui, D., Zhou, C., Ren, Q, 2011. Mesoporous silica-coated gold nanorods with embedded indocyanine green for dual mode X-ray CT and NIR fluorescence imaging. Optics Express, 19, 17030.

Martín-García, B., Paulo, P.M.R., Costa, S.M.B., Velázquez, M.M, 2013. Photoluminescence Dynamics of CdSe QD/Polymer Langmuir–Blodgett Thin Films: Morphology Effects. The Journal of Physical Chemistry C, 117, 14787-14795.

Martini, N., Koukou, V., Fountos, G., Valais, I., Bakas, A., Ninos, K., Kandarakis, I., Panayiotakis, G., Michail, C, 2018. Towards the enhancement of medical imaging with non-destructive testing (NDT) CMOS sensors. Evaluation following IEC 62220-1-1:2015 international standard. Procedia Structural Integrity, 10, 326-332.

Martini, N., Koukou, V., Fountos, G., Valais, I., Kandarakis, I., Michail, C., Bakas, A., Lavdas, E., Ninos, K., Oikonomou, G., Gogou, L., Panayiotakis, G, 2019. Imaging performance of a $CaWO_4$/CMOS sensor. Frattura ed Integrità Strutturale, 13(50), 471-480.

Michail, C., Fountos, G., Liaparinos, P., Kalyvas, N., Valais, I., Kandarakis, I., Panayiotakis, G, 2010. Light emission efficiency and imaging performance of Gd_2O_2S:Eu powder scintillator under X-ray Radiography conditions. Medical Physics, 37(7), 3694-3703.

Michail, C., Kalyvas, N., Bakas, A., Ninos, K., Sianoudis, I., Fountos, G., Kandarakis, I., Panayiotakis, G., Valais, I., 2019. Absolute Luminescence Efficiency of Europium-Doped Calcium Fluoride (CaF_2:Eu) Single Crystals under X-ray Excitation. Crystals, 9(5), 234.

Michail, C., Karpetas, G., Kalyvas, N., Valais, I., Kandarakis, I., Agavanakis, K., Panayiotakis, G., Fountos, G, 2018. Information Capacity of Positron Emission Tomography Scanners. Crystals, 8(12), 459.

Michail, C., Valais, I., Fountos, G., Bakas, A., Fountzoula, C., Kalyvas, N., Karabotsos, A., Sianoudis, I., Kandarakis, I, 2018. Luminescence Efficiency of Calcium Tungstate ($CaWO_4$) under X-ray radiation: Comparison with Gd_2O_2S:Tb. Measurement, 120, 213-220.

Michalet, X, 2005. Quantum Dots for Live Cells, in Vivo Imaging, and Diagnostics. Science, 307, 538-544.

Nikolopoulos, D., Valais, I., Michail, C., Bakas, A., Fountzoula, C., Cantzos, D., Bhattacharyya, D., Sianoudis, I., Fountos, G., Yannakopoulos, P., Panayiotakis, G, 2016. Kandarakis, I. Radioluminescence properties of the CdSe/ZnS Quantum Dot nanocrystals with analysis of long-memory trends. Radiation Measurements, 92, 19-31.

Öberg, V.A., Zhang, X., Johansson, M.B., Johansson, E.M.J, 2017. Solution-Processed Environmentally Friendly Ag_2S Colloidal Quantum Dot Solar Cells with Broad Spectral Absorption. Applied Sciences, 7, 1020.

Okeke, C., Thite, A., Durodola, J., Greenrod, M, 2019. Fatigue life prediction of Polymethyl methacrylate (PMMA) polymer under random vibration loading. Procedia Structural Integrity, 17, 589-595.

Public Health England, Cadmium: Health Effects, Incident Management nd Toxicology Information On Cadmium, For Responding To Chemical Incidents [Online]. Available: https://www.gov.uk/government/publications/cadmium-properties-incident-management-and-toxicology, Published 1 July 2014 Last updated 25 October 2016.

Rauch, T., Böberl, M., Tedde, S.F., Fürst, J., Kovalenko, M.V., Hesser, G., Lemmer, U., Heiss, W., Hayden, O, 2009. Near-infrared imaging with quantum-dot-sensitized organic photodiodes. Nature Photonics, 3, 332-336.

Saatsakis, G. Kalyvas, N. Michail, C. Ninos, K. Bakas, A. Fountzoula, C. Sianoudis, I. Karpetas, G.E. Fountos, G. Kandarakis, I. Valais, I. Panayiotakis, G, 2019. Optical Characteristics of ZnCuInS/ZnS (Core/Shell) Nanocrystal Flexible Films Under X-Ray Excitation. Crystals, 9, 343.

Saatsakis, G., Michail, C., Fountzoula, C., Kalyvas, N., Ninos, K., Bakas, A., Sianoudis, I., Kandarakis, I., Fountos, G., Panayiotakis, G., Valais, I., 2019. Luminescence Efficiency of Zn-Cu-In-S / ZnS Quantum Dot films, IEEE Xplore, 1-4, doi: 10.1109/DTIS.2019.8734940.

Saatsakis, G., Michail, C., Fountzoula, C., Kalyvas, N., Bakas, A., Ninos, K., Fountos, G., Sianoudis, I., Kandarakis, I., Panayiotakis, G. Valais, I, 2019. Fabrication and luminescent properties of Zn-Cu-In-S / ZnS Quantum Dot films under UV excitation. Applied Sciences, 9(11), 2367.

Saatsakis, G., Valais, I., Michail, C., Fountzoula, C., Fountos, G., Koukou, V., Martini, M., Kalyvas, N., Bakas, A., Sianoudis, I., Kandarakis, I., Panayiotakis, G, 2017. Preliminary Study of ZnS:Mn^{2+} Quantum Dots Response Under UV and X-Ray Irradiation. Journal of Physics Conference Series, 931, 012030.

Seferis, I.E., Michail, C., Zeler, J., Kalyvas, N., Valais, I., Fountos, G., Bakas, A., Kandarakis, I., Zych, E., Panayiotakis, G.S, 2018. Detective quantum efficiency (DQE) of high X-ray absorption Lu_2O_3:Eu thin screens: the role of shape and size of nano- and micro-grains. Applied Physics A, 124, 604.

Seferis, I.E., Zeler, J., Michail, C., Valais, I., Fountos, G., Kalyvas, N., Bakas, A., Kandarakis, I., Zych, E, 2016. On the response of semitransparent nanoparticulated films of $LuPO_4$:Eu in poly-energetic X-ray imaging applications. Applied Physics A, 122, 526.

Son, D.I., Kwon, B.W., Park, D.H., Seo, W.-S., Yi, Y., Angadi, B., Lee, C.-L., Choi, W.K, 2012. Emissive ZnO-graphene quantum dots for white-light-emitting diodes. Nature Nanotechnology, 7, 465-471.

Stodilka, R.Z., Carson, J.J.L., Yu, K., Zaman, M.B., Li, C., Wilkinson, D, 2009. Optical Degradation of CdSe/ZnS Quantum Dots upon Gamma-Ray Irradiation. The Journal of Physical Chemistry C, 113, 2580-2585.

Thomson, L.A., Law, F.C., James, K.H., Matthew, C.A., Rushton, N, 1992. Biocompatibility of particulate polymethylmethacrylate bone cements: a comparative study in vitro and in vivo. Biomaterials, 13, 811-818.

Valais, I., Michail, C., Fountzoula, C., Fountos, G., Saatsakis, G., Karabotsos, A., Panayiotakis, G, Kandarakis, I, 2017. Polymer Based Thin Film Screen Preparation Technique, Journal of Physics Conference Series, 931, 012035.

Valais, I., Michail, C., Fountzoula, C., Tseles, D., Yannakopoulos, P., Nikolopoulos, D., Bakas, A., Fountos, G., Saatsakis, G., Sianoudis, I., Kandarakis, I Panayiotakis, G, 2017. On the response of alloyed ZnCdSeS quantum dot films. Results in Physics, 7, 1734-1736.

Wu, T., Sher, C.-W., Lin, Y., Lee, C.-F., Liang, S., Lu, Y., Huang Chen, S.-W., Guo, W., Kuo, H.-C., Chen, Z, 2018. Mini-LED and Micro-LED: Promising Candidates for the Next Generation Display Technology. Applied Sciences, 8, 1557.

Yu, W.W., Chang, E., Drezek, R., Colvin, V.L, 2006. Water-soluble quantum dots for biomedical applications. Biochemical and Biophysical Research Communications, 348, 781-786.

Zeler, J., Cybinska, J., Zych, E, 2016. A new photoluminescent feature in $LuPO_4$:Eu thermoluminescent sintered materials. RSC Advances, 6, 57920.

Zych, E., Meijerink, A., Donega, C, 2003. Quantum efficiency of europium emission from nanocrystalline powders of Lu_2O_3:Eu. Journal of Physics: Condensed Matter, 15, 5145-5155.